Journal of the Korean Nuclear Society
Volume 32, Number 4, pp.299~308, August 2000

An Assessment of Reactor Vessel Integrity Under In-Vessel Vapor Explosion Loads

Kwang-Hyun Bang, Jong-Rae Cho
Korea Maritime University
1 Dongsam-dong Yeongdo-gu, Pusan 606-791, Korea
khbang@hanara.kmaritime.ac.kr

Soo-Yong Park
Korea Atomic Energy Research Institute
150 Dukjin-dong Yusong-gu, Taejon 305-353, Korea

(Received September 4, 1999)

Abstract

A safety assessment of reactor vessel lower head integrity under in-vessel vapor explosion loads has been performed. The core melt relocation parameters were chosen within the ranges of physically realizable bounds. The premixing and explosion calculations were performed using TRACER-II code. Using the calculated explosion pressures imposed on the lower head inner wall, strain calculations were performed using ANSYS code. Then, the calculated strain results and the established failure criteria were used in determining the failure probability of the lower head. In the explosion analyses, it is shown that the explosion impulses are not altered significantly by the uncertain parameters of triggering location and time, fuel and vapor volume fractions in uniform premixture bounding calculations. Strain analyses show that the vapor explosion-induced lower head failure is not possible under the present framework of assessment. The result of static analysis using the conservative explosion-end pressure of 50 MPa also supports the conclusion. It is recommended, however, that an assessment of fracture mechanics for preexisting cracks be also considered to obtain a more concrete conclusion.

Key Words : vapor explosion, fuel-coolant interaction, severe accident, reactor vessel

1. Introduction

In present day light water reactors, if complete and prolonged failure of normal and emergency coolant flow occurs, fission product decay heat could cause melting of the reactor fuel. If the molten fuel mass accumulates it may relocate into reactor lower plenum and if the lower head fails it may eventually be brought into the reactor cavity. In such course of core melt relocation, the opportunity for fuel-coolant interactions (FCIs) arises as the core melt relocates into water pool

in-vessel as well as ex-vessel and also, as a consequence of implementing accident management strategies involving water addition to a degraded or molten core.

In the course of a severe accident, a broad range of FCI phenomena is possible due to the variations in reactor geometries, core degradation scenarios, and timing and mode of fuel-coolant contact. In the TMI-2 accident[1], a slow and dripping flow of molten core into a deep water pool through a largely open lower plenum occurred and led to quenching of core melt and formation of a coolable debris bed. On the other hand, upon a catastrophic failure of the crust by which large quantity of melt is supported in the core region, a rapid and massive release of melt may occur followed by its relocation to the lower plenum. Though such massive relocation does not imply that the entire amount of melt participates in energetic FCI, even a fractional amount may lead to a highly energetic vapor explosion and consequent pressure loading on reactor vessel and surrounding structures.

If the amount of melt involved in a vapor explosion inside the reactor vessel is large enough and the resulting mechanical energy release is sufficiently large, the explosion may fail the reactor upper head, throwing it upward, hitting the containment ceiling, consequently posing a potential risk of containment failure. This is so-called vapor explosion induced containment failure (α-mode failure)[2]. For years reactor safety analysts have studied the probability of the α-mode containment failure and have reached a tentative consensus on that the α-mode containment failure is not risk significant[3].

The in-vessel retention (IVR) strategy, employed in advanced light water reactors with passive design features, is based upon external cooling of the reactor vessel through cavity flooding. To assure the success of the IVR strategy, the potential for an early failure of the lower head from in-vessel vapor explosions must be ruled out. This new accident management strategy of in-vessel retention in advanced light water reactors has directed the risk potential of in-vessel vapor explosions from the α-mode containment failure to the reactor lower head failure.

One of the advanced light water reactors which first employed the in-vessel retention strategy was the AP600 of Westinghouse. Theofanous et al.[4] studied systematically on the assessment of lower head integrity under in-vessel steam explosion loads in an AP600-like reactor design. The assessment included the evaluation of melt conditions and timing of release from the core region, mixing and explosion wave dynamics, and lower head fragility. Mixing and explosion calculations were performed using PM-ALPHA and ESPROSE.m-3D codes and strain analysis of lower head was made using ABAQUS code. The major conclusion was that steam-explosion-induced lower head failure in an AP600-like reactor is physically unreasonable.

The objective of this study is to perform a safety assessment of the reactor lower head integrity of a Korea Next Generation Reactor (KNGR)-like PWR under the in-vessel vapor explosion loads. The initial conditions of melt relocation into the lower plenum were provided by the bounding approximation within the physically realizable ranges. The premixing and explosion calculations were performed using TRACER-II code[5,6], and the strain calculations of the reactor lower head under the dynamic explosion pressure loads were performed using ANSYS code[7]. The framework of the assessment is shown in Fig. 1. The core melt relocation parameters were chosen within the ranges of physically realizable bounds and also of conservative results. The triggering time and locations were varied and the resulting explosion loads were compared to determine the significant

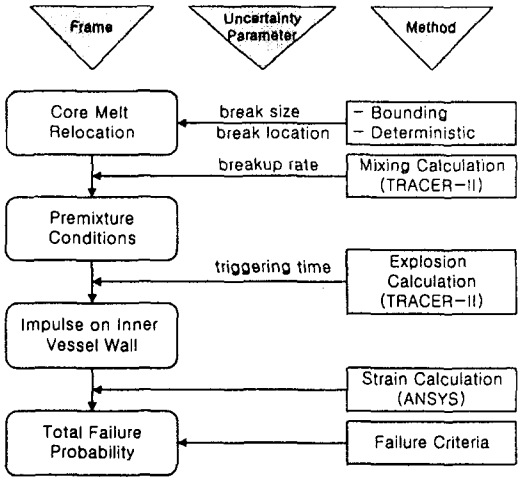

Fig. 1. Framework of Lower Head Integrity Assessment

cases. Using the calculated explosion loads, strain calculations were performed, and then the calculated strain results and the established failure criteria were used in determining the failure probability of the lower head.

2. In-Vessel Vapor Explosion Loads

To assess the integrity of reactor vessel under the in-vessel vapor explosions, a systematic evaluation of the course of core melt-coolant interactions is required from the melt relocation to the structural response of the vessel lower head under dynamic pressure impulse imposed on the inner wall. In light water reactors such as KNGR, a broad range of FCI phenomena is possible due to the variations in reactor geometries, core degradation scenarios, and timing and mode of fuel-coolant contact. A slow and dripping flow of molten core into a deep water pool through a largely open lower plenum may lead to quenching of core melt and formation of a coolable debris bed.

On the other hand, upon a catastrophic failure

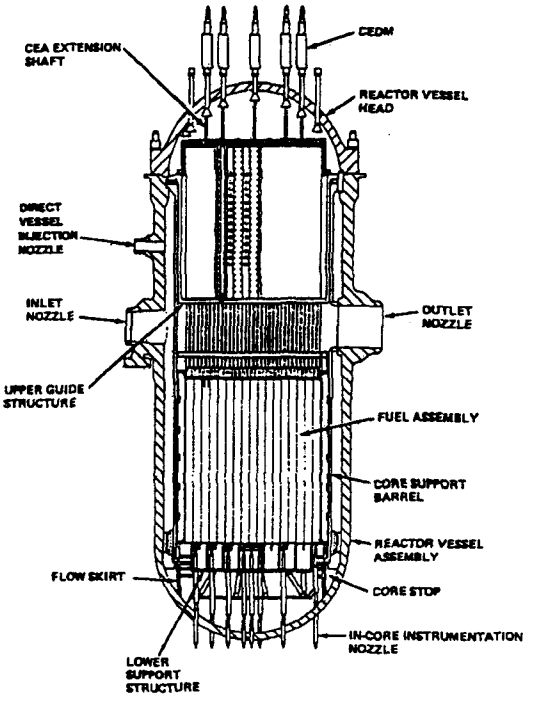

Fig. 2. Schematic of a KNGR-like Reactor Vessel

of the crust by which large quantity of melt is supported in the core region, a rapid and massive release of melt may occur followed by its relocation to the lower plenum. Though such massive relocation does not imply that the entire amount of melt participates in energetic FCI, even a fractional amount may lead to a highly energetic vapor explosion and consequent pressure loading on reactor vessel and surrounding structures. Furthermore, the crowded lower plenum with core support structures and in-core instrumentation guide tubes such as in KNGR tends to make the FCI behavior more complicated, although such crowded lower plenum may have a mitigating effect to highly energetic vapor explosions.

A schematic view of the lower plenum of a KNGR-like PWR is shown in Fig. 2. The inner diameter of the lower head is 4.74 m and the vessel thickness is 165 mm at minimum. The

Table 1. Material Properties of Corium Used in the Analyses

Constituents	UO_2	ZrO_2	Zr	S.S.	Corium
Weight fraction, %	75.2	11.4	8.5	4.9	100
Melt temp., K	3,138	2,963	2,141	1,700	~3,000
Molar frac., %	50.7	16.6	16.6	16.1	100
Volume frac., %	66.3	16.6	10.8	6.3	100
Density, kg/m^3	8,700	~5,250	~6,000	6,000	7,660
Specific heat, J/kgK	500	710	364	777	526
Ther. cond., W/mK	3.66	2.3	31.5	22	8.5
Viscosity, kg/ms	0.0043	~0.004	~0.005	0.007	0.005
Surface tension, N/m	0.5	0.5	~1.5	1.5	0.5
Heat of fusion, kJ/kg	278	700	251	261	323

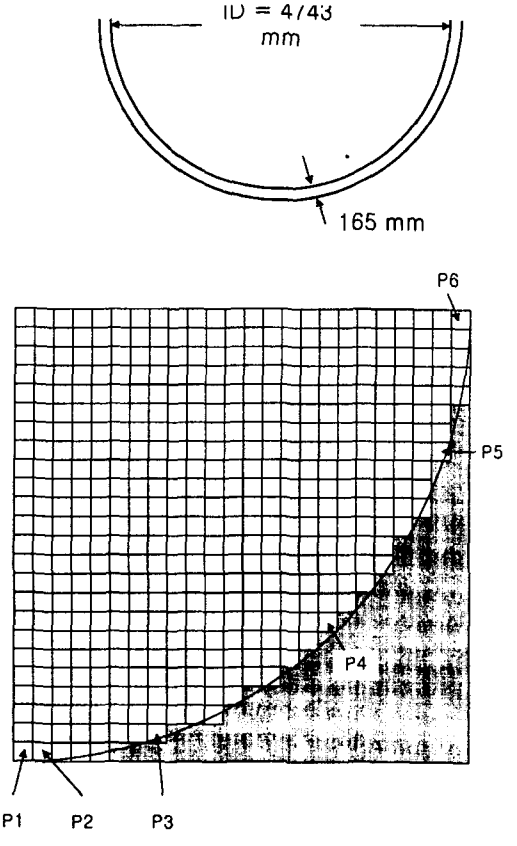

Fig. 3. 24 × 24 Nodalization of Reactor Lower Head

lower plenum is occupied by lower support structure and in-core instrumentation guide tubes. In this study, it is assumed that the lower plenum is empty, hemispherical. The support structures and in-core instrumentation guide tubes are not considered. However, one notes that such crowded lower plenum may have a mitigating effect on explosion energetics. The size and position of melt relocation are generally uncertain parameters due to the variations in core degradation scenarios. In this study, the relocation parameters were chosen within the range of physically reasonable contents and also for conservative results.

The in-vessel vapor explosion analysis provides dynamic pressure impulses imposed on the inner wall of lower head for the strain analysis. In order to provide a conservative results, two groups of calculations were performed; (1) under the assumption of uniform premixture throughout the lower plenum, explosion calculations were performed with the variation of trigger position and magnitude, and fuel and vapor volume fractions within the range of physically realistic bounds. (2) a single jet of melt enters lower plenum filled with coolant. In this case, premixing and subsequent explosion propagation calculations were performed with the variation of triggering time after the melt entry.

The calculations were performed using

TRACER-II code. It is a two-dimensional code capable of cartesian and cylindrical coordinates. The lower plenum is treated as an axisymmetrical hemisphere in cylindrical coordinates by treating the nonphysical part as solid volumes as shown in Fig. 3. The number of nodes were 24 in axial direction and 24 in radial direction for a 2.40 m-radius lower head. Therefore, the size of one control volume is 10 cm × 10 cm. The labels of P1 to P6 in Fig. 3 indicate the selected positions of inner wall of lower head for presenting calculated explosion pressure traces. The reader refers these labels when identifying the positions in the related figures. The material properties of corium[8] used in this analysis are as given in Table 1.

2.1. Effect of Triggering in Uniform Premixture

The base fuel volume fraction of assumed uniform premixture is 0.2. This is equivalent to 44 tons of fuel, which can be a reasonable upper bound within the physically realistic melt relocation. The base vapor volume fraction in this set of calculations is 0.1. The variation of the triggering point is the bottom or the top of the polar axis of the lower plenum. And, two triggering pressures were evaluated: 10 MPa and 1 MPa, although it is generally believed that the magnitude of this artificial triggering pressure, a common technique for a triggering in computation of vapor explosion, is not a controlling parameter for explosion energetics once the explosion propagates and escalates.

The case of bottom triggering shows gradual pressure arrival along the lower head inner wall as shown in Fig. 4. However, the top triggering imposes the pressure on the wall almost at the same time as expected. Also, it was shown that the trigger pressure of 1 MPa does not change the overall pressure traces. In all cases, a level of about

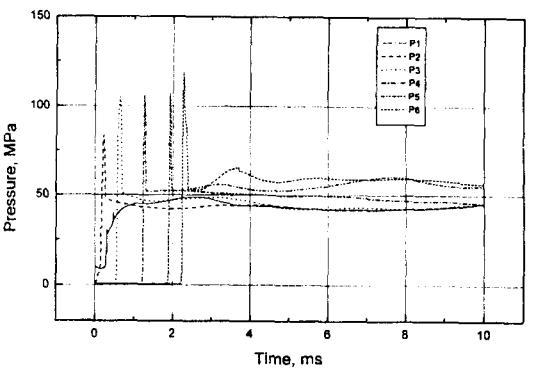

Fig. 4. Explosion Pressures in Uniform Mixture (10 MPa, Bot. Trig., α_f=0.2, α_g=0.1)

50 MPa of explosion pressures were sustained after a sharp peak reaching 125 MPa. This implies that the triggering pressure or location does not alter the overall impulse on the lower head.

2.2. Effect of Volume Fractions in Uniform Premixture

The fuel volume fraction was varied from 0.1 to 0.3, which corresponds to 22 tons to 66 tons of core. The vapor volume fraction was varied from 0.05 to 0.2. The base case of fuel fraction of 0.2 and vapor fraction of 0.1 is shown as in Fig. 4.

The results of fuel volume fraction variation in uniform premixture show that the higher fuel content tends to increase the propagation speed, but rather decrease the peak pressure. This reduction of peak pressure is due to the smaller amount of coolant liquid available when the fuel content increases. In these cases also, the end-state pressure level and the overall impulse are not generally altered by the variation of fuel volume fraction within the range of the present study.

The results of vapor volume fraction variation in uniform premixture show that the lower vapor content tends to increase the propagation speed

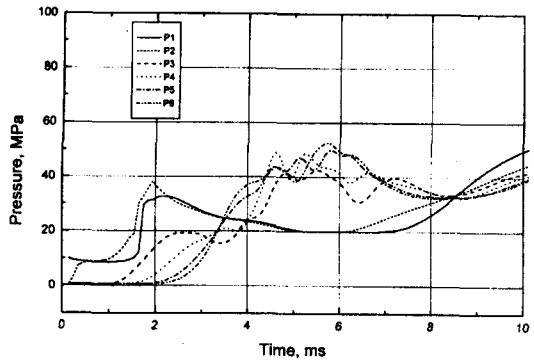

Fig. 5. Explosion Pressures in 30 cm Jet at Center (0.7 s Mixing Time after Injection)

and the peak pressure and the higher vapor content tends to decrease the propagation speed as well as the peak pressure. However, the end-state pressure level and the overall impulse are not generally altered by the variation of vapor volume fraction within the range of the present study.

2.3. Effect of Trigger Time in Single-jet Relocation

The melt jet enters at the center of lower plenum and the diameter of the jet is 30 cm in the present analysis. The entering speed of the jet is 3.0 m/s. The triggering pressure is 10 MPa and the location is the bottom. The triggering time after the melt entry was varied from 0.3 s to 0.7 s. The result of mixing calculation shows that the melt leading front hit the bottom at about 0.5 s after the injection. The pressure traces at selected points of the lower head inner wall for 0.7 s triggering time are shown in Fig. 5. As compared to Fig. 4, the peak pressures and the overall impulses are much lower than those of the case of uniform premixture.

After evaluating the significance of the parameters in overall explosion impulses, some selected pressure traces were used in the strain analyses as given in the following section.

3. Assessment of Reactor Vessel Integrity

In developing a methodology for assessing likelihood of lower head failure under millisecond-duration pressure pulses with peaks in the kilobar range, it is very important to characterize and understand the dynamics due to axisymmetrically distributed highly transient loads to strain hardening effects on material constitutive behavior. Lower head integrity under steam explosion loads is analyzed by use of the finite element method. The assessment includes the comprehensive evaluation of explosion wave dynamics and lower head fragility under local, dynamic loads.

3.1. Failure Criteria

It is evident that lower plenum venting and associated energy dissipation will strongly depend on the time and location of the lower head failure. Considerable effects was, therefore, devoted to exploring the range of behavior predicted through the application of various existing failure criteria.

Failure criteria used by Bohl and Butler[9] as well as by Berman et al.[10] were phenomenologically based on continuum mechanics. Each criterion was based on equivalent plastic strain, $\overline{\varepsilon_p}$, which is defined in terms of the principal plastic strains as

$$\overline{\varepsilon_p}=\frac{\sqrt{2}}{3}\left[(\varepsilon_1-\varepsilon_2)^2+(\varepsilon_2-\varepsilon_3)^2+(\varepsilon_3-\varepsilon_1)^2\right] \quad (1)$$

According to Bohl and Butler, failure should occur at ~12% equivalent plastic strain. Berman et al. on the other hand, placed this criterion at ~18%.

Failure criteria for ductile materials, as is the case here, have most commonly been based on plastic equivalent strains, with typically conservative values in the 13 to 18% range[11]. All experimental evidences, however, and

theoretical interpretations indicate that failure is not obtained until much greater strains, say in the 50 to 100% range.

The potential effect of strain rate on failure has been examined with conflicting results. On the one hand, Johnson and Cook[12] have provided an expression for the strain at failure in terms of five material-dependent parameters. In general, the strain at failure increases with temperature and strain rate. On the other hand, Shockey et al.[13] in the A533B tests explored strain rates of up to 1,000 s^{-1}, and concluded that there is no effect of temperature or strain rate on failure.

The failure criteria will have to be evaluated conservatively. For this purpose, the mechanistic ideas of ductile failure based on void nucleation, growth, and with particular reference to the work of Shockey et al. were used. It was found that voids nucleate predominantly on included particles, and that the threshold strain of 11% is needed for nucleation. In applying these ideas to the present situation with a highly nonuniform distribution of plastic equivalent strains across the wall thickness, the global wall failure likelihood can be related to the fraction of wall thickness experiencing strain that support nucleation, as indicated in Table 2[14].

3.2. Results and Discussion

The geometric modeling of the lower head was performed by ANSYS version 5.3[7]. The lower head is modeled by 4-node axisymmetric solid elements. The number of nodes is 140 and the number of elements is 114. Material of the lower head is SA508 class 3 steel, and assumed as an elastic-linear plastic behavior ignoring strain hardening effects, and the following material properties are used at 260℃:

Young's modulus, E = 186 GPa

Poisson's ratio, ν = 0.3

Yield stress, σ_y = 345 MPa

Allowable stress intensity, Sm = 207 MPa

Tangent modulus, E_T = 1,620 MPa

For the boundary conditions, horizontal displacement is restrained for the nodes on the top of head., and vertical displacement is restrained for the nodes on the bottom of head.

As a reference case, a static analysis of vessel lower head was performed for the design pressure of 17.2 MPa. In this case, the maximum membrane stress intensity is 161 MPa at junction of the top of the head and the shell and the membrane stress intensity at a section is 121 MPa and is less than the allowable value of 207 MPa. The maximum equivalent strain is 0.1% and is much less than the allowable value of 11%.

The transient dynamic analysis of explosion load was performed using a selected set of calculated time histories of explosion pressures. In Case I, explosion pressure applies uniformly on the whole inside of the lower head. In Case II, the inside surface of the head is divided by 6 segments, and various history of explosion pressure applies on the each segments (e.g., Fig. 4).

In Case I, the maximum equivalent strain is 0.11% at 0.01 s of explosion load. The maximum

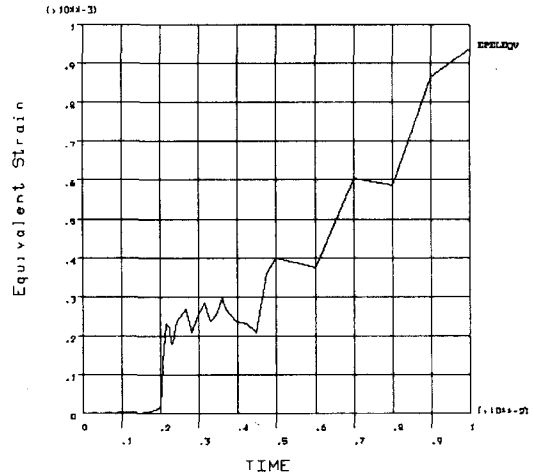

Fig. 6. Time History of Equivalent Strain

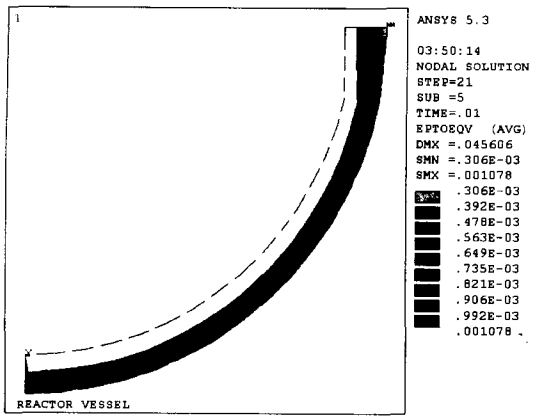

Fig. 7. Contour of Equivalent Strain

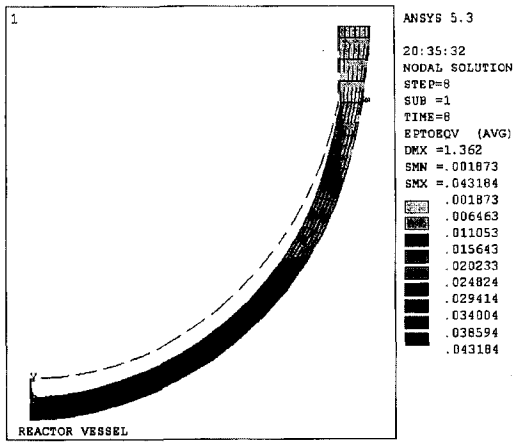

Fig. 8. Contour of Equivalent Strain in 50 MPa Static Condition

Table 2. Quantification of Wall Failure Criteria[14]

Likelihood	Wall Fractional Thickness with Plastic Equivalent Strain over 11%	Probability
Physically Unreasonable	First Fiber	$<10^{-3}$
Outside of Spectrum	20%	10^{-2}
Edge of Spectrum	40%	10^{-1}
Certain Failure	60%	10^{0}

membrane stress intensity is 115 MPa and the maximum membrane plus bending stress is 156 MPa. For Case II, the time history of equivalent strain is shown in Fig. 6. Contour of the equivalent strain at 0.01 s is shown in Fig. 7. The maximum equivalent strain is 0.108%. The maximum membrane stress intensity is 110 MPa and the maximum membrane plus bending stress is 146 MPa.

It is noted that in the above two cases, equivalent stress and strain continue to increase with time. This is because the explosion pressures in these cases have long plateau since all the lower head walls are assumed closed for conservative result. Therefore, in Case III, the long plateau of explosion-end pressure is applied continuously on the inner side of lower head. The pressure is 50.0 MPa. The maximum equivalent stress in this case is 389 MPa and is greater than the yield stress of 345 MPa. A contour of the equivalent strain is shown in Fig. 7. The maximum equivalent strain is 4.3% at the bottom of lower head. Because the equivalent strain of 4.3% is less than 11% threshold that support nucleation according to Table 2, it can be concluded that the possibility of lower head failure does not exist.

4. Conclusions

The reactor vessel lower head integrity under in-vessel vapor explosion loads has been studied. The core melt relocation parameters were chosen within the ranges of physically realizable bounds. The premixing and explosion calculations were performed using TRACER-II code. The triggering time and locations were varied and the resulting

explosion pressures were compared for determining the most significant cases. Using the calculated explosion pressures imposed on the lower head inner wall, strain calculations were performed using ANSYS code. Then, the calculated strain results and the established failure criteria were used in determining the failure probability of the lower head.

The explosion analyses show that the explosion impulses are not altered significantly by the uncertain parameters of triggering location and time, fuel and vapor volume fractions in uniform premixture bounding calculations within the conservative ranges. Strain analyses using the calculated pressure loads on the lower head inner wall show that the vapor explosion-induced lower head failure is not possible under the present framework of assessment. Even, the static analysis using the conservative explosion-end pressure of 50.0 MPa shows that the maximum equivalent strain is 4.3% at the bottom of lower head. Because the equivalent strain of 4.3% is less than the allowable threshold value of 11% in the fragility model used here, the possibility of the lower head failure under in-vessel vapor explosion loads does not exist. It is recommended, however, that an assessment of fracture mechanics for preexisting cracks be also considered to obtain a more concrete conclusion.

In this study, it is assumed that the lower plenum is empty, hemispherical, although it is occupied by lower support structures and in-core instrumentation guide tubes in a KNGR-like reactor. The crowded lower plenum tends to make the FCI behavior more complicated, although such crowded lower plenum may have a mitigating effect to highly energetic vapor explosions. The area of in-core instrumentation guide tube penetration may be more fragile under explosion loads, but an assessment requires an analytical tool which is capable of three-dimensional calculation of vapor explosions as well as a local strain analysis with detail structural and welding conditions of the penetrations. The assessment of the fragility of the in-core instrumentation guide tube penetrations is, therefore, suggested when a necessary set of calculational tools are available in the future for a complete and comprehensive assessment of reactor lower head integrity under in-vessel vapor explosion loads.

Acknowledgement

This work was supported by the Korea Electric Power Co. through the Korea Atomic Energy Research Institute and the Electrical Engineering and Science Research Institute.

References

1. J.R. Wolf and J.L. Rempe, "TMI-2 Vessel Investigation Project," TMI V(93)EG10, INEL Report (1993).
2. USNRC, "Reactor Safety Study," WASH-1400, NUREG/75-0114, Oct. (1975).
3. S. Basu and T. Ginsberg, "A Reassessment of the Potential for an Alpha-Mode Containment Failure and a Review of the Current Understanding of Broader Fuel-Coolant Interaction Issues," Report of 2nd SERG, NUREG-1524 (1996).
4. T.G. Theofanous, W.W. Yuen, S. Angelini, J.J. Sienicki, K. Freeman, X. Chen and T. Salmassi, "Lower Head Integrity under Steam Explosion Loads," Proc. of the OECD/CSNI Specialists Meeting on Fuel-Coolant Interactions, Tokai-Mura, Japan, Vol. II, 63-118, May (1997).
5. K.H. Bang, I.K. Park, G.C. Park, "TRACER-II: A Complete Computational Model for Mixing and Propagation of Vapor Explosions," Proc. of the OECD/CSNI

Specialists Meeting on Fuel-Coolant Interactions, Tokai-Mura, Japan, Vol. II, 804-816, May (1997).
6. I.K. Park, "A Computational Model for the Mixing and Propagation of Vapor Explosions," Ph.D Thesis, Seoul National University (1998).
7. ANSYS Users Manual, Swanson Analysis System Inc. (1985).
8. M.L. Corradini et al., "FCI Experiments and Analysis: Contributions to Basic Understanding," Proc. of the OECD/CSNI Specialists Meeting on Fuel-Coolant Interactions, Tokai-Mura, Japan, Vol. II, 609-622, May (1997).
9. W.R. Bohr and T.A. Butler, "Comments on Proposed Research Contributing to the Relation of Residual Steam Explosion Issues," Letter Report in "A Review of Current Understanding of the Potential for Containment Failure Arising from In-Vessel Steam Explosion," NUREG-1116, U.S. Nuclear Regulatory Commission, Feb. (1985).
10. M. Berman, D.V. Swenson and A.J. Eickett, "An Uncertainty Study of PWR Steam Explosions," SAND83-1438, NUREG/CR-3369, Sandia National Laboratories, May (1984).
11. W.H. Amarasooriya and T.G. Theofanous, "An Assessment of Steam-Explosion-Induced Containment Failure. Part III: Expansion and Energy Partition," Nuclear Science & Engineering, 97, 296-315 (1987).
12. G.R. Johnson and W.H. Cook, "Fracture Characteristics of the Metals Subjected to Various Strains, Strain Rates, Temperatures and Pressures," Engineering Fracture Mechanics 21, 31-48 (1985).
13. D.A. Shockey, L. Seaman, K.C. Dao and D.R. Curran, "Kinetics of Void Development in Fracturing A533B Tensile Bars," J. Pressure Vessel Technology 102, 14-21 (1980).
14. T.G. Theofanous, W.W. Yuen, S. Angelini, J.J. Sienicki, K. Freeman, X. Chen and T. Salmassi, "Lower Head Integrity under Steam Explosion Loads," Proc. of the OECD/CSNI Specialists Meeting on Fuel-Coolant Interactions, Tokai-Mura, Japan, Vol. II, 63-118, May (1997).